RESEARCH PAPER

Modular micro-robotic assembly through magnetic actuation and thermal bonding

Eric Diller · Naicheng Zhang · Metin Sitti

Abstract We present and compare new heat-activated bonding methods for use in modular micro-robotic systems. Such modular systems prove to provide on-demand creation of arbitrary micro-scale physical shapes in remote inaccessible spaces. The bonding methods presented here quickly form strong bonds through the use of thermoplastic or solder binding sites integrated into each module face, addressing problems of assembly strength and electrical conductivity. The strength of the bonds for each method are presented for different module styles, bonding conditions and breaking conditions in a destructive test, and are compared with previous magnetic bonding methods. For 80 micrometer modules, bond strengths of up to 500 mN are observed with thermoplastic bonds, which indicates that the assemblies could be potentially used in high-force structural applications of programmable matter, microfluidic channels or healthcare. Using previously-developed micro-robot addressing methods, magnetically-functionalized modules are moved remotely for assembly using a magnetic coil system. In this way, a set of up to nine modules are remotely assembled one-by-one into an arbitrary shape capable of locomotion to demonstrate the scalability and strength of the system.

1 Introduction

Recent work in reconfigurable robotics has involved the scaling down of individual robotic modules for increased resolution and access to small spaces. This has brought with it several challenges in actuation, computation, and module bonding [24]. Many large-scale modular robotic systems use traditional actuators such as dc motors [26] or shape memory alloys [25] to power the assembly, reconfiguring, motion, and disassembly processes using algorithms or motion primitives [16, 22]. However, as these systems are scaled down below the centimeter-scale, compromises must be made which reduce functionality, resulting in modules with less mobility. While these problems could be addressed for some purposes by using a subtractive reconfiguration strategy with limited actuation [8], such a system has limitations such as a lack of mobility, and a purely passive assembly scheme. A few approaches to micro-scale modular systems have presented actuation solutions at the sub-millimeter scale using directed [19] or stochastic [20] fluid flow or magnetic actuation [5]. Electrostatically-driven scratch-drive micro-robotic actuators have been shown to assemble in 2D without bonding [7]. These actuation schemes have proved useful, and could be extended to more complex systems with many modules.

E. Diller (✉) · N. Zhang · M. Sitti
5000 Forbes Ave., Scaife Hall 307,
Pittsburgh, PA 15213-3890, USA
e-mail: ediller@andrew.cmu.edu

N. Zhang
e-mail: naicheng@seas.upenn.edu

M. Sitti
e-mail: sitti@cmu.edu

In contrast with self-assembly or other bulk fabrication techniques, robotic micro-assembly is deterministic in nature, and involves the introduction of discrete robotic elements for in-situ assembly. Depending on the application area, desirable capabilities for micro-scale modular robot assemblies could include, as illustrated in Fig. 1:

– Small module size
– Physical presence (large assembly size)
– Addressable modules
– Creation of arbitrary 2D/3D shapes
– Mechanical strength
– Electrical conductivity/continuity
– Reconfiguration
– Disassembly

While the first steps towards reconfiguration and disassembly have been demonstrated with magnetic bonding [5], the other desired capabilities are relatively unaccomplished. The creation of assemblies with physical presence has been shown to some extent, but is limited to two dimensions (2D), and with a limited number of modules. Mechanical strength and electrical conductivity have not been demonstrated. Thus, this paper presents a bonding method which offers mechanical strength, could allow for extension to 3D out-of-plane physical presence, and has potential to allow electrical conductivity between modules.

Low-strength bonding methods for the structural bonding of micro-scale assemblies have been shown to some extent previously. As one approach, Tolley et al. fabricated micro-scale silicon modules which snap together using flexural hooks [19]. Such hooks could be difficult to fabricate and align, and may not provide large bonding strength. Magnetic bonding is commonly used in centimeter-scale and larger
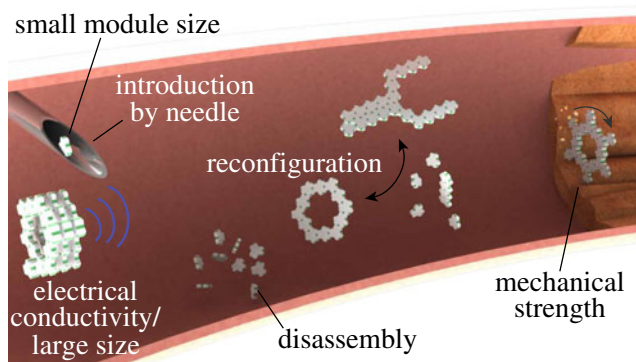

Fig. 1 Micro-scale modular robot concept. Shown are some of the desired capabilities of a modular system for microfluidic, programmable matter or healthcare applications. Modules are introduced through a small opening, shown here as a needle. They can then reconfigure and disassemble into various shapes. On the far left is an electrical element such as a coil, and on the far right, a strong structure for grinding

reconfigurable robotic modules [21], and has been demonstrated previously for micro-scale bonding [5]. While these micro-scale magnetic modules show promise for reconfigurable assemblies, magnetic force scales with magnetic volume, so the attractive force at the micro-scale becomes very weak.

We propose a heat-activated bonding method for micro-scale reconfigurable modules in which the modules themselves are passive. Heat is applied in one of two ways: global conduction through the surrounding liquid or localized heating by focused laser. Global conduction uses an electrical heating element embedded in the workspace to activate all bonding sites simultaneously while laser heating is accomplished by a focused laser system for fast and accurate heating at a single bonding site. As a long-term solution for inaccessible environments such as inside the human body, inductive heating by AC magnetic fields [17] could be used, but is not implemented in this work due to the requirements for specialized high power equipment. A similar method has been used as a micro-gripper at the tip of a tethered end-effector by solidifying the liquid surrounding the tip [18], but has not been shown in an untethered system.

We also introduce a new magnetic addressing method for the independent untethered control of a large number of modules. We have shown several methods for magnetic addressing of small groups of micro-robotic modules for 2D [1] or 3D [2] motion. However, here we use a scalable addressing method which allows for larger groups to be controlled through selective magnetic disabling [3, 4]. This method will allow for an arbitrary number of modules to be added to an assembly, without requirements for a specialized operating environment. Such addressing methods are critical for micro-scale reconfigurable robotic assemblies.

Structurally sound micro-assemblies could have major advantages in areas of microfluidics or healthcare where a large structure must be introduced in a minimally invasive manner. Medical procedures involving occlusions, stents or ablation in the cardiovascular system could benefit from modular micro-robot assemblies which are introduced via needle injection, assemble in-situ for treatment, and can be broken apart afterward for removal [14]. Other potential applications could be for in-situ heterogeneous tissue scaffold construction or in microfluidic channels for fluid or cell manipulation.

Preliminary results of this study were presented in ref. [6]. Here we give additional experimental results and the critical addition of a magnetic addressability method for multi-module control which we show can also be used for magnetic disassembly. The paper is structured as follows. Section 2 provides an overview of the experimental control and fabrication techniques used. Section 3 provides results of bond strength measurement. Section 4 presents results

from the use of magnetic disabling for addressable control of assembling modules and Section 5 concludes the paper.

2 Experimental setup

2.1 Module design and fabrication

2.1.1 Thermoplastic bonding modules

Modules with bonding sites are fabricated in a multi-step molding process, as outlined in Fig. 2. First, a polyurethane module with embedded magnetic composite particles is fabricated in a batch process using a micro-molding technique using SU-8 photolithography, as presented in [5]. They are composed of a mixture of neodymium-iron-boron (NdFeB) particles (Magnequench MQP-15-7) suspended in a polyurethane matrix (TC-892, BJB enterprises). The shape was chosen as roughly hexagonal to allow tessellation of many modules in 2D. Curved edges are used to aid in alignment of adjacent faces prior to bonding. The module has voids along its edges of approximate size several hundred μm, as shown in Fig. 2a, which will ultimately become the binding sites. As a low-temperature thermoplastic for

bonding, commercially available Ethylene-vinyl acetate hot-melt adhesive is used. These adhesives are available with a variety of properties, including different melting temperatures. To fill the binding sites with thermoplastic material in a controlled manner, the module is placed in a soft rubber jig designed to match the shape of the module without voids, as in Fig. 2b. A photograph of 18 modules in the jig setup is shown in Fig. 2e. The thermoplastic is then deposited under high temperature (130 °C) to melt into the voids, bubbles are removed by placing in a vacuum chamber, and the remaining material is scraped clean using a sharp edge, as shown in Fig. 2c. After cooling, the module is removed from the jig and is ready for bonding with other modules under low heat (approximately 70 °C), as in Fig. 2d. A photograph showing two pairs of bonded modules is shown in Fig. 2f, demonstrating the reliable fabrication and bonding.

2.1.2 Solder bonding modules

Modules with solder bonding sites are fabricated in a similar manner to the thermoplastic bonding modules, with the thermoplastic replaced by low-melting point metal. This procedure is shown in Fig. 2g-i. To permit the solder to wet

Fig. 2 Multi-step molding process. **a** Module and jig prior to bonding site filling. **b** The module is placed in the jig. **c** The thermoplastic is deposited under high temperature (130 °C) to melt into the voids. Vacuum is applied while hot to remove air bubbles in the voids. **d** After cooling, the module is removed from the jig and is ready for bonding with other modules. **e** Photograph of 18 modules in the jig, prior to the addition of thermoplastic. **f** Photograph showing two pairs of bonded hexagonal modules. **g** To create solder-bond modules, copper is first sputtered onto the module surfaces. **h** Solder is then applied manually using tweezers at 90 °C. **i** The modules are now prepared and ready to bond with other modules under temperatures of about 70 °C
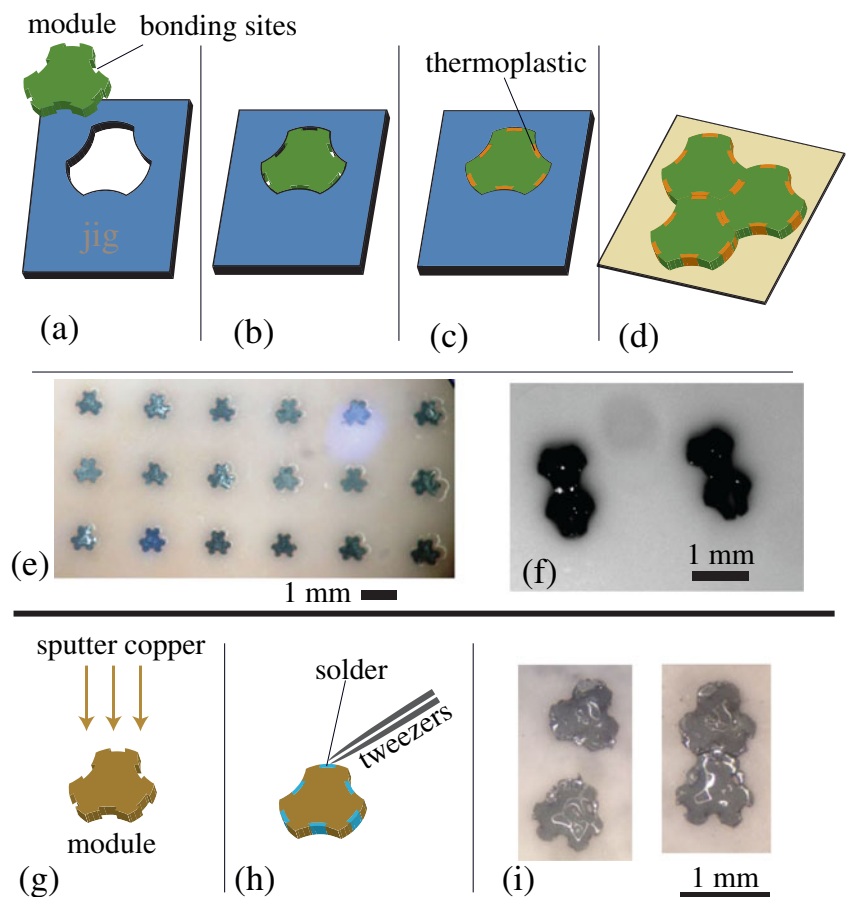
the the module, copper is sputtered onto the top and bottom polyurethane surface. Some copper is deposited into the binding sites on the side of the modules during this sputtering. The solder is then applied manually to each bonding site using tweezers in an optical microscope at 80 °C. An indium alloy (Field's metal) is used as low melting temperature solder, with a sharp melting point of about 62 °C. This metal fuses well with itself at high temperature, when in air, water or oil.

2.1.3 Magnetic bonding modules

Bonding by magnetic attraction alone is a simple method which follows naturally from the use of magnetically-actuated modules. This method is widely used in large-scale robotics, was investigated for micro-scale robotic elements in detail in our previous work [5], and has the major advantage of being an easily reversible bond. However, the major limitation is that the bonding strength is low, and it requires special out-of-plane module geometry to resist contact sliding and rotation, as the magnetic force provides no interface shear strength. In addition, modules can only be bonded in a limited number of magnetically stable configurations. The most stable shapes are long straight chains, although some other geometries can be assembled, albeit with a lower bonding strength. Magnetic modules are fabricated using the same methods used to make the thermoplastic and solder modules, but without the bonding sites. As the bonding strength is dependent on the magnetic moment of the modules, a strong magnetic moment is necessary.

2.2 Actuation and heating

Module bonding occurs by heating to temperatures around 50–90 °C, depending on the bonding material. As many potential applications of micro-robots occur in liquid environments, all experiments are conducted in silicone oil or water. One heating approach involves raising the temperature of the entire liquid volume. This method has the advantage of simplicity, and does not require precise knowledge of the module locations. However, it melts all bonding sites in the workspace, and takes a longer time to heat and cool than other methods. It also required mechanical access to the workspace area. An experimental setup has been created to heat the workspace liquid by electrothermal heating. This setup, shown in Fig. 3a, b, is based around a well of water or oil on a glass slide, which forms the experimental workspace. Underneath the glass slide is glued a Peltier heating element, heated by a 1.0 A power supply. In the experiments in this paper, the water temperature is monitored by a thermocouple, and is assumed constant over the water volume due to the thin water layer and the high thermal conductivity of water when compared with the air
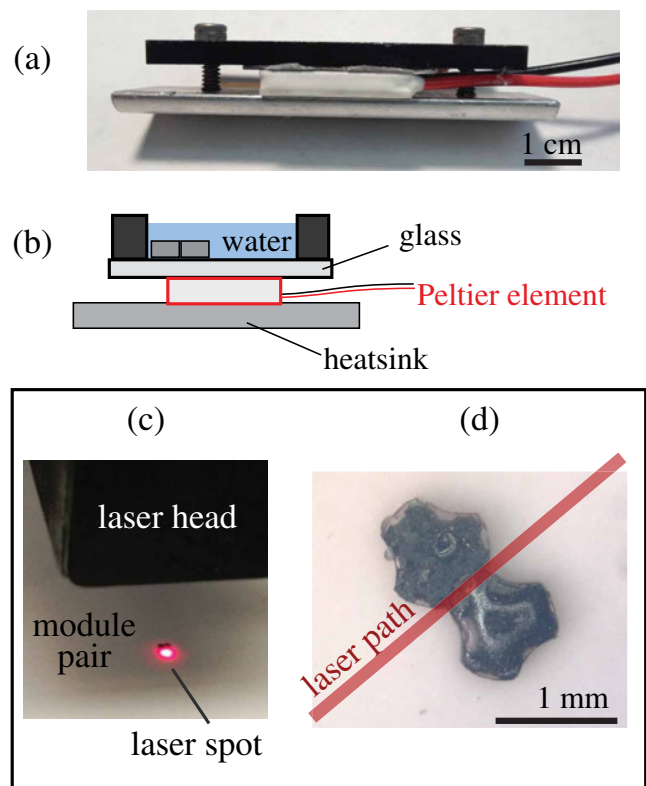

Fig. 3 Heating methods. **a** Photograph of the heating setup by Peltier element. The workspace is contained in the top dark layer of acrylic. **b** Schematic of the layers of the heating experiment. **c** Heating by focused laser. **d** The laser path crosses the site to be bonded, leaving other bonding sites relatively unaffected

above it. Once the desired bonding temperature is reached, the heating current is removed or reversed and the system cools to room temperature, at which point adjacent modules are bonded together. For a thin 2 mm water layer, heating from 30 °C to 70 °C with 1 A takes approximately 12 sec while cooling takes approximately 30 sec with no current applied. Larger volumes of liquid take a longer duration to heat and cool. Heating by electrical means is used as the primary method in this paper due to its simplicity and precise temperature control capability.

Laser heating is a second possible method which would achieve fast, localized bonding. This method could be integrated into an experimental setup for targeted bonding of only a single glue site pair. As a proof-of-concept demonstration of this method, a commercial CO_2 laser (Pinnacle V-Series Laser Engraver, 35 W) is used to bond two modules, as shown in Fig. 3c, d. Here the laser power is approximately 3 W with a spot size of approximately 100 μm, and is traced across the module bond at a speed of 0.55 m/s four times with a spacing of 0.5 s. This power provides enough heat to bond the modules without damaging the polyurethane module base.

As a third potential method for heating, inductive heating by high-power AC fields could be used remotely without a line-of-sight to the modules. While inductive heating of magnetic particles and particle suspensions have been studied [9], achieving the desired temperature rise of over 15 °C could be a practical challenge with this method, especially as the module size is reduced below hundreds of micron size.

2.3 Motion actuation

Magnetic modules are actuated by a set of independent electromagnetic coils, aligned pointing towards a common center point, with an open space of approximately 10.4 cm. The coils are operated with an air or iron core, depending on the desired magnetic fields and gradients. The maximum fields produced by the system driven at maximum current (19 A each) are 6.6 kA/m using air cores, and 19.4 kA/m using iron cores. Similarly, maximum field spatial gradients are 271 A/m^2 using air cores, and 812 A/m^2 using iron cores. Fields are measured using a Hall effect sensor (Allegro A1321) with an error of about 80 A/m. Control of the currents driving the electromagnetic coils are performed by a PC with data acquisition system at a control bandwidth of 20 kHz, and the coils are powered by linear electronic amplifiers (SyRen 25). A photograph of the experimental coil system is shown in Fig. 4.

2.3.1 Magnetic influences

Magnetic modules can be controlled by the magnetic coils surrounding the workspace, and also interact with each other. The total magnetic torque ($\overrightarrow{T}$) and force ($\overrightarrow{F}$) that govern these interactions are:

$$\overrightarrow{T} = \mu_0 \overrightarrow{m} \times \overrightarrow{H} \tag{1}$$

$$\overrightarrow{F} = \mu_0 (\overrightarrow{m} \bullet \overrightarrow{\nabla}) \overrightarrow{H} \tag{2}$$

for a module with magnetic moment $\overrightarrow{m}$, where $\overrightarrow{H}$ is the total magnetic field from the coils or nearby modules and $\mu_0 = 4\pi \times 10^{-7}$ H/m is the permeability of free space. Magnetic interaction forces between modules are investigated in-depth in Diller et al. [5].

The magnetic field and its spatial gradients depend linearly on the currents through the coils [10], and so the field and gradient terms can be expressed as

$$\overrightarrow{H} = \mathbf{H} \overrightarrow{I}, \tag{3}$$

$$\frac{\partial \overrightarrow{H}}{\partial x} = \mathbf{H}_x \overrightarrow{I}; \quad \frac{\partial \overrightarrow{H}}{\partial y} = \mathbf{H}_y \overrightarrow{I}; \quad \frac{\partial \overrightarrow{H}}{\partial z} = \mathbf{H}_z \overrightarrow{I}, \tag{4}$$
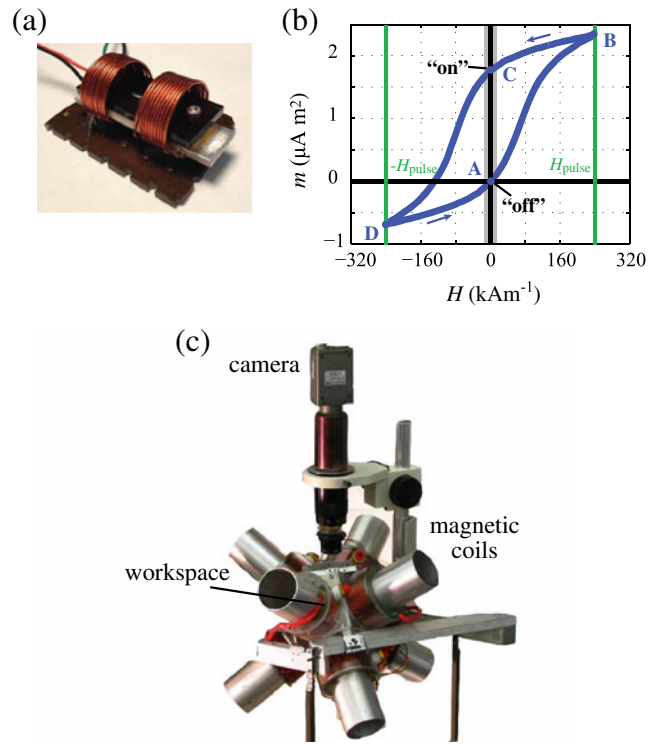
Fig. 4 Experimental heating and actuation setup. **a** The Peltier-based heating assembly is placed inside a low-inductance pulsing magnetic coil for magnetic disabling of individual modules. **b** Magnetic disabling response of a magnetic composite module. **c** This assembly is then placed inside the larger actuation coil system. The workspace is surrounded by magnetic coils to allow for remote actuation of the magnetic modules. Module motion is observed using a top-view camera and microscope

where each element of $\overrightarrow{I}$ is current through each of the c coils, $\mathbf{H}$ is a $3 \times c$ matrix mapping these coil currents to the magnetic field vector $\overrightarrow{H}$ and $\mathbf{H}_x$, $\mathbf{H}_y$, $\mathbf{H}_z$ are the $3 \times c$ matrices mapping the coil currents to the magnetic field spatial gradients in the x, y and z directions, respectively. These mapping matrices are calculated for a given coil arrangement by treating the coils as magnetic dipoles in space and are calibrated through workspace measurements as outlined in [10, 12].

Thus, for a desired field and force on a single magnetic micro-robot we arrive at

$$\begin{bmatrix} \overrightarrow{H} \\ \overrightarrow{F} \end{bmatrix} = \begin{bmatrix} \mathbf{H} \\ \overrightarrow{m}^T \mathbf{H}_x \\ \overrightarrow{m}^T \mathbf{H}_y \\ \overrightarrow{m}^T \mathbf{H}_z \end{bmatrix} \overrightarrow{I} = \mathbf{A} \overrightarrow{I}, \tag{5}$$

where $\mathbf{A}$ is the $6 \times c$ matrix mapping the coil currents $\overrightarrow{I}$ to the field $\overrightarrow{H}$ and force $\overrightarrow{F}$. These equations can be solved for the coil currents $\overrightarrow{I}$ from a desired field and force. In this way, we can achieve 5 DOF control of magnetic modules, enabling motion on 2D surfaces for assembly tasks as will be shown in the experimental demonstrations at the

end of the paper. Motion is accomplished by rolling, direct pulling or by vibration-based stick-slip crawling, methods which have been demonstrated previously [15, 23]. Feedback control of single or teams of micro-robots moving in 3D are not fully exploited in this work, but the feasibility of such control has been shown in our previous studies [2].

2.4 Module addressing by magnetic disabling

Remotely and selectively turning on and off the magnetization of individual modules could allow for addressable control of each module. We have developed a composite material whose net magnetic moment can be selectively turned on or off by application of a large magnetic field pulse [4, 13]. The material is made from a mixture of micron-scale neodymium-iron-boron and ferrite particles, and can be formed into arbitrary actuator shapes using the simple molding procedure discussed in Section 2.1.1. The magnetic coercivity and remanence (retained magnetization value when the applied field H is reduced to zero) are distinct, which allows for moderately-large fields to re-magnetize the ferrite while maintaining the NdFeB magnetization. By applying a pulse in the desired direction greater than the coercivity field (H_c) of the ferrite, its magnetization direction can be switched instantly. In addition, the magnetic states of both NdFeB and ferrite can be preserved when driving an actuator using small fields of less than 12 kA/m.

In general it is difficult to demagnetize a single magnet by applying a single demagnetizing field because the slope of the hysteresis loop (i.e. the magnetic permeability) near the demagnetized state is very steep. Thus, such a demagnetization process must be very precise to accurately demagnetize a magnet. While steadily decreasing AC fields can be used to demagnetize a magnetic material, this method does not allow for addressable demagnetization because it will disable all magnets in the workspace. This motivates the use of a magnetic composite to enable untethered addressable magnetic disabling.

We employ a demagnetization procedure to achieve a more precise demagnetization by employing two materials, both operating near saturation where the permeability is relatively low. In this method, an applied switching field H_{pulse} can be applied to switch only one material's (ferrite) magnetization without affecting the second material (NdFeB). As the two materials are mixed in one magnetic module, this switching allows the device to be switched between on and off states as the magnetic moments add in the on state or cancel in the off state. While the internal field of the magnet at any point will not be zero, the net field outside the magnet will be nearly zero, resulting in negligible net magnetic actuation forces and torques.

When fields are applied below the NdFeB coercivity, the NdFeB acts as a permanent magnet, biasing the device magnetization, as shown in Fig. 4b for H_{pulse} up to about 240 kA/m. Traversing the hysteresis loop, the device begins in the off state at point A, where motion actuation fields, indicated by the 12 kA/m range, only magnetize the device to about 0.08 μAm^2, resulting in minimal motion actuation. To turn the device on, a 240 kA/m pulse is applied in the forward direction, bringing the device to point B. After the pulse, the device returns to point C, in the on state. Here, motion actuation fields vary the device moment between about 1.7 and 1.8 μAm^2. To turn the device off, a pulse in the backward direction is applied, traversing point D, and returning to the off state at point A at the conclusion of the pulse. For small motion actuation fields in the lateral direction, the device is expected to show even lower permeability in the on or off state due to the shape anisotropy induced during the molding process.

Thus, modules can be magnetically disabled by a short field pulse of high strength. This will allow for multiple modules to be added to an assembly at a time and sequentially disabled. As the process is reversible, the modules can be re-enabled magnetically once the assembly process is complete, allowing for the entire assembly to be actuated.

3 Bond characterization

Module bonding strength is measured in a destructive test which pulls two modules directly apart while measuring the loading force using a load cell, as shown in Fig. 5a. The module pair is glued to a 3-axis motion stage with manual linear motion. The 'loading beam' is placed on the load cell and a fulcrum, and serves to reduce the force transmitted to the load cell, as shown schematically in the figure inset. The modules are first glued on a removable plastic tip by instant adhesive. Then the tip is fixed on the motion stage and aligned manually using the camera such that the modules come into contact with the loading beam, which is coated in a thin layer of adhesive. When the adhesive has cured, the motion stage is lowered at a constant rate until the bond between the modules breaks. The load cell data is acquired by amplifier/conditioner (TMO-2) and DAQ at a rate of 10 kHz. To get the breaking force, the difference between the maximum value during the breaking and the value of zero load after the break is calculated, as shown in Fig. 5b. Calibration is made by a 20 g proof mass placed at the same position on the loading beam in a separate measurement. The bond breaking phase is not instantaneous due to the viscoelastic nature of the thermoplastic at elevated temperatures.
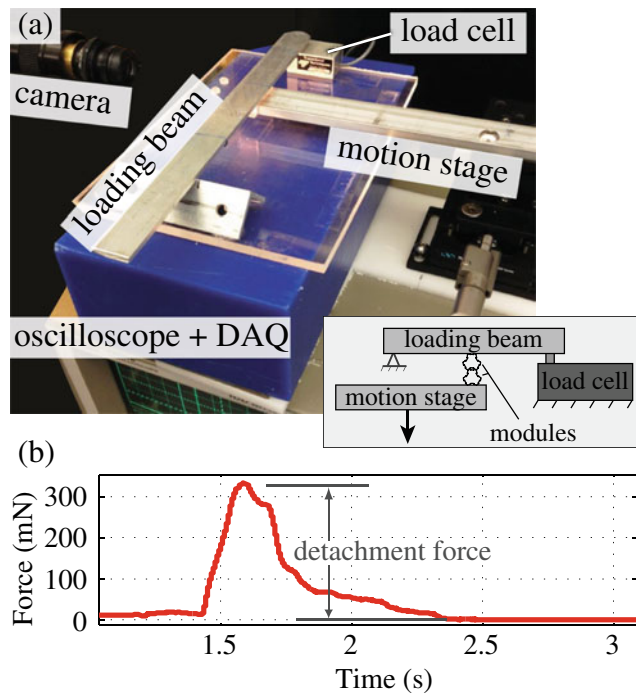
Fig. 5 Bonding strength test setup. **a** Force measurement setup using a load cell, where the bonded modules are pulled apart until they detach. **b** Example force versus time plot for a thermoplastic bond, style 'D', broken at room temperature. The max force is taken as the detachment force
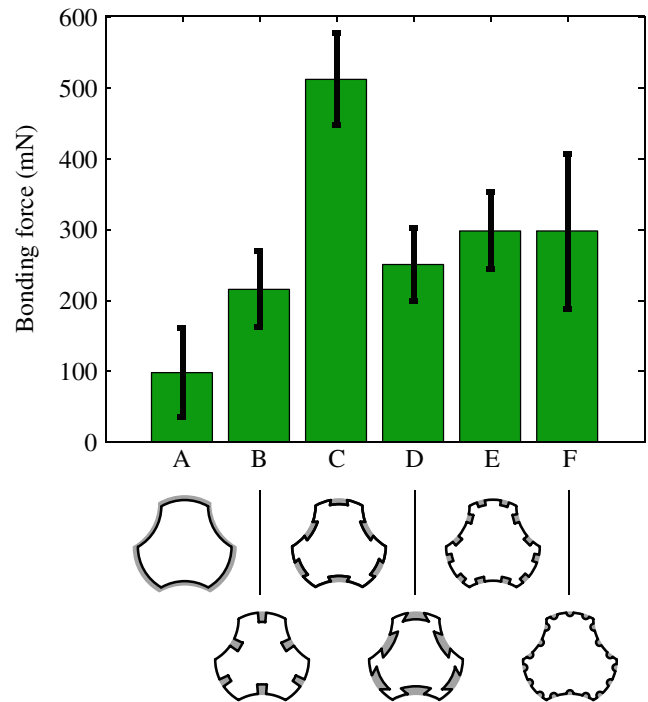

Fig. 6 Comparison of different glue bonding site styles broken at room temperature. The mean bonding force of each module style is shown in the bar graph, with the styles shown below each data point. Error bars show standard deviation for five trials

3.1 Bonding types

Representative thermoplastic, solder, and magnetic bonding module pairs are compared with respect to bonding force, with results shown in Table 1. Module 'style' refers to the size, number and shape of the bonding sites, and can be referenced in Fig. 6. This table shows the mean and standard deviation in force for five module pairs for each type of test. Modules assembled by hand are pushed together using tweezers in a microscope and then heated. Those assembled by "coils" are pushed together in the magnetic coil system using magnetic force on one module while the second module remains in place. Assembly by hand using tweezers is also directly compared with assembly using magnetic forces in the magnetic coil system, showing that while hand

assembly can result in larger bond force, the coil-assembled pairs maintain an adequate force. Bonding by laser was only performed for one module pair as a proof-of-concept demonstration due to the difficulty in aligning the laser in the current setup. Results for solder bonding show moderate bond force, where it is noted that the failure mode is the delamination of the solder with the copper seed layer rather than failure of the bulk solder. As expected, magnetic bonding is by far the weakest bonding style, but has the advantage of easily reversible bonding.

3.2 Bonding face style

For thermoplastic bonds, the bonding faces of each module contain voids for thermoplastic to reside. By varying the number, shape and size of these voids, different bonding strengths are achieved, with results shown in Fig. 6 for five samples of each face style. Six styles of module with the same outer diameter size of $800 \mu m$ but different bonding faces are designed and fabricated for direct comparison. Below the bar graph, the polyurethane module body is shown in white while the thermoplastic is shown in grey. To obtain a thin layer of thermoplastic in style 'A' with no voids, the $800 \mu m$ module is placed into a jig with diameter of $810 \mu m$. All other module styles are prepared in a jig

Table 1 Comparison of bonding forces

Bond Type	Style	Assembly	Bonding Force (mN)
Thermoplastic	D	hand	246 ± 55
Thermoplastic	D	coils	168 ± 54
Thermoplastic	D	hand/laser	87
Solder	D	hand	172 ± 27
Magnet	A	hand	2.7 ± 1.6

of size 800 μm. Results in the bar graph show the advantages of using dedicated thermoplastic voids over the 'A' style. This indicates that the design of bonding faces with voids has improved the bonding force between modules from approximately 100 mN to several hundred mN. It is seen that all void styles show adequate bond force, but the single-void of wide size but shallow depth (style 'C') shows the highest bond force. It is expected that the wider bonding site increases the bond strength as it should depend primarily on cross-sectional bond area, but the depth of style 'D' prevents it from having high adhesion as the glue needs to penetrate deep into the recess to adhere fully. Thus, while it is determined that any module style with voids results in acceptable bond force, further study could improve the bond force even further through optimized void style. It is thus desired to increase the cross-sectional bond area while maintaining full glue penetration.

3.3 Bonding temperature

To determine the required temperature to form a secure bond, the breaking force of thermoplastic module pairs bonded under different temperatures is investigated, with results shown in Fig. 7a. Here heat is applied carefully to each 'C'-style module pair using a heat gun in an air environment. The temperature at the bonding site is monitored using a thermocouple. After cooling to room temperature, each module pair is mounted in the destructive test shown in Fig. 5 for breaking at 22 °C. Results show that a critical temperature of about 55 °C is necessary to form a bond. Module pairs indicated with 0 bonding force achieved no bonding at all, as indicated by them not being able to support their own weight when lifted with tweezers. At temperatures above 55 °C, high bonding force is relatively consistent (with one failed bond at 65 °C). However, above about 80 °C the thermoplastic melts to such a degree that it flows from the bond sites. While this can allow for high bonding force, the geometry of the module pair is distorted by the pool of thermoplastic which forms around the base of the modules. The duration of heating was not observed to have an effect on bond strength.

The strength of a thermoplastic bond broken at high temperature is investigated in Fig. 7b, where identical modules bonded at 70 °C are broken at varying temperatures. High temperature during the break test is achieved using a Peltier thermoelectric element, driven by 1 A current, and monitored with a thermocouple glued to the Peltier element face near the module pair. The plot shows that for temperatures lower than about 40 °C, the bond force is high and relatively insensitive to temperature. However, at higher temperatures the bond force is lower. The bond force never reduces to zero due to the strong capillary and visco-elastic nature of the melted thermoplastic. The results from both
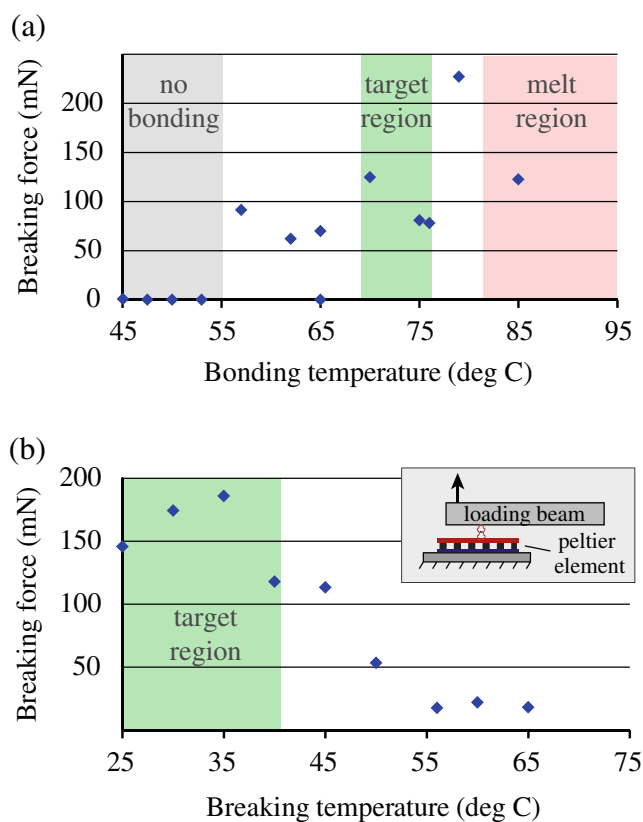

Fig. 7 Dependence of thermoplastic bond force on temperature, for module style D. **a** Force as a function of temperature during bonding. All modules are broken at a temperature of 22 °C. **b** Force as a function of temperature during module breaking. All modules are bonded at a temperature of 70 °C

of these temperature tests are specific to the thermoplastic used.

3.4 Assembly and bonding demonstration

A demonstration to show the bonding of 2D tessellating shapes is shown in Fig. 8. Here, six 'F' thermoplastic modules are moved in the magnetic coil system for assembly in Fig. 8. Modules are bonded by applying heat using the integrated resistive heating setup shown in Fig. 4. The inset in Fig. 8b shows the capillary drawing action which pulls adjacent modules into intimate contact during the reflow process. In this experiment, only one module is magnetic, allowing for step-by-step addition of the non-magnetic modules. When the assembly is moved adjacent to a new module, heat is applied to bond it to the assembly. This proves that subsequent bonding cycles can be performed in the presence of existing bonds at other sites without negative effect. The single magnetic module is able to carry the non-magnetic modules, although when the assembly reaches a size of five modules, as in Fig. 8e, the mobility is somewhat reduced, making it more difficult to precisely
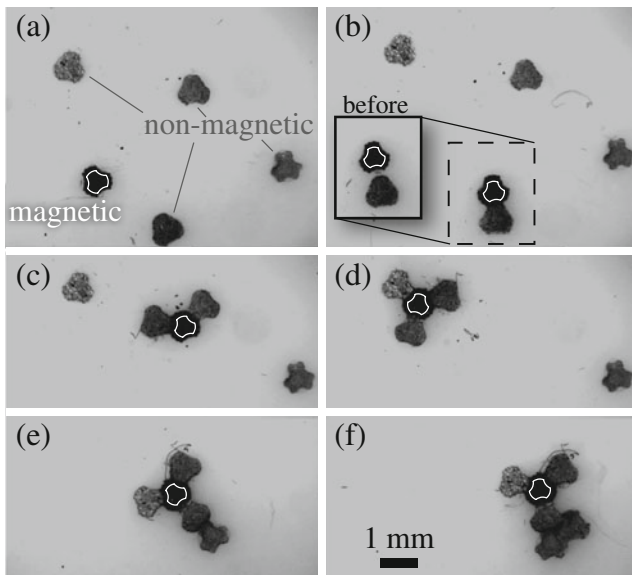
Fig. 8 Bonding demonstration, showing six modules bonded by thermoplastic bonding in the magnetic coil setup. The single magnetic module is moved to pick up the non-magnetic modules one-by-one. At each step, the temperature is briefly increased to 70 °C once the modules are close. The inset in (**b**) shows the configuration before heat is applied, and demonstrates how the modules are naturally pulled close by capillary force when the thermoplastic is melted. Video available in Supplementary Materials

add more modules to the assembly in the desired configuration. However, the large assembly is still very mobile using the methods of stick-slip crawling or tumbling cartwheel-like rolling motion. The bond force is high enough that the assembly is not broken by moving in the coil system under magnetic torques and forces, even when the temperature is elevated to 70 °C.

4 Disabling for module addressability

To add more magnetic modules to an assembly, each module is magnetically disabled after assembly, as shown schematically in Fig. 9. This process allows individual modules to be added to the assembly one at a time into arbitrary locations on the assembly without regard for the magnetic attraction or repulsion associated with that assembly location. Compared with bonding by magnetic attraction, this allows for a much wider range of assembly morphologies to be made. New modules can be added to the assembly in any position or orientation. However, it is desirable to bond all modules with the same orientation so that they can be disabled and enabled as a group using a single global pulse. Heat bonding of modules is accomplished by individual heating (i.e. by laser or inductive heating), or by global heating (i.e. heat conduction through the entire medium).
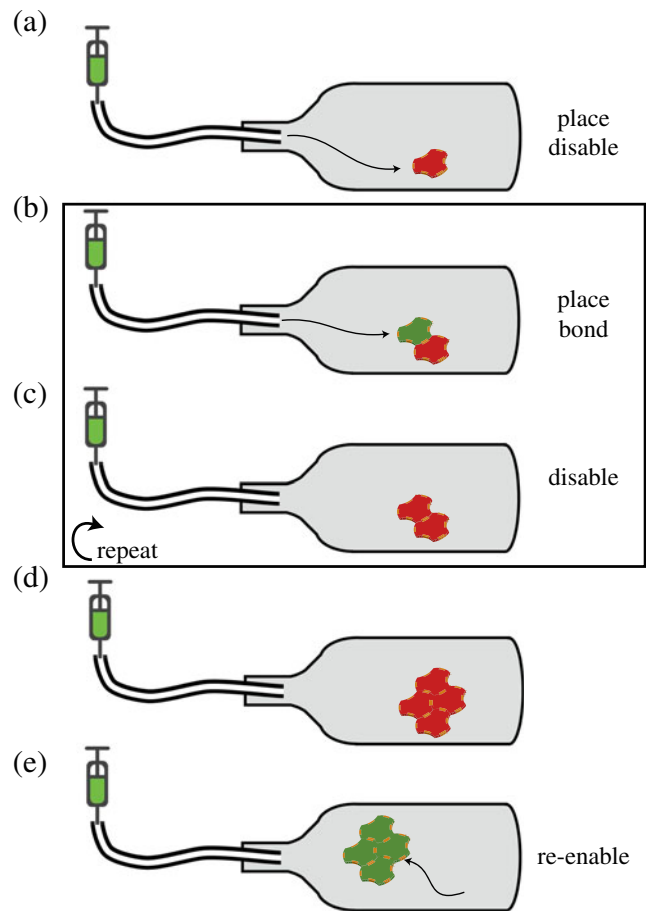

Fig. 9 Method for combining multiple magnetic modules in one assembly using thermal bonding. **a** Individual modules are added one at a time through the confined environment opening. After the module is placed, it is magnetically disabled using a magnetic field pulse. **b-c** As new modules are added, they are placed, bonded magnetically and then disabled. This allows subsequent modules to be bonded into any target location on the assembly without regard for magnetic attraction or repulsion. **d** The assembly is complete. **e** The entire assembly is re-enabled magnetically and is then free to move as a single unit by magnetic propulsion

Once the assembly is completed, it is re-enabled magnetically and is free to move through the workspace as a single unit.

As further demonstration of the assembly plus heat-activated bonding, a 2D ship-in-bottle morphology is created in a microfluidic chip environment, as shown in Fig. 10. Creating a ship in a bottle requires individual modules to pass through a small opening (the bottle neck) and assemble into a ship shape one at a time. The simple 2D ship shape made here consists of nine modules, and consists of a hull, mast and sail. Such a demonstration shows the capability of the presented addressability, bonding and control method to achieve the creation of arbitrary shapes in remote inaccessible areas. The assembled ship is enabled magnetically by a magnetic pulse for actuation as a rigid body. The strength
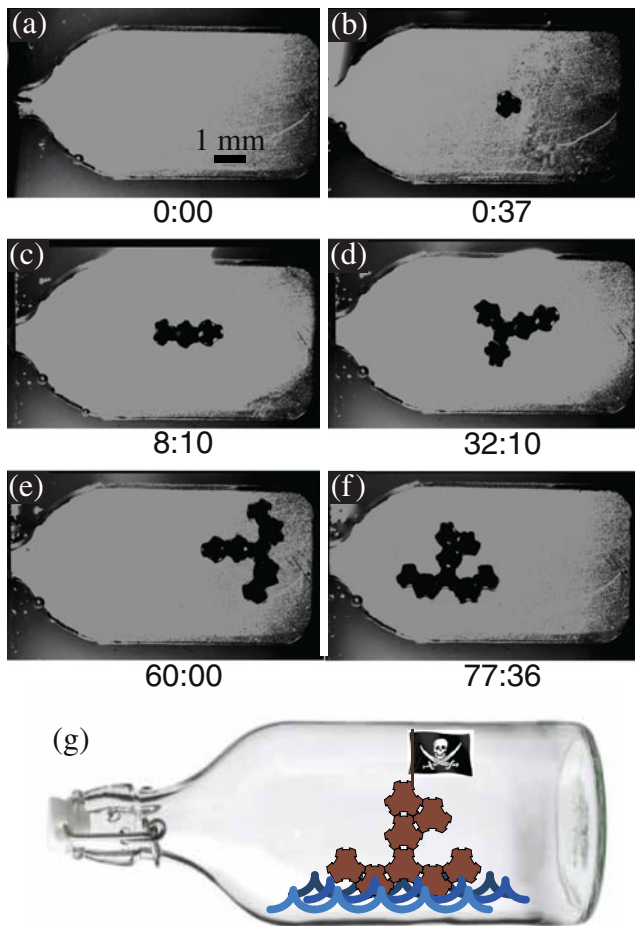
Fig. 10 Bonding demonstration, showing nine modules bonded by thermoplastic bonding in the magnetic coil setup. The operating environment is 20 cSt silicone oil, and the bottom surface is aluminum coated with teflon coating. The "bottle" walls are made from laser-cut acrylic and is covered with glass cover slip. The system is heated in the same manner as the previous setups. Experiment time stamps are shown as minutes:seconds. **a-f** Modules are added, bonded and disabled sequentially to form a ship shape. **g** The completed ship is magnetically enabled and moves through the bottle as a single object. Video available in Supplementary Materials

of the assembly is demonstrated by fast actuation after it is assembled, and is promising for future physical interactions with the environment.

4.1 Disabling for magnetic disassembly

A final study is conducted using magnetic disabling to show that magnetic module bonds can be broken directly. While we have demonstrated that magnetic bonds are much weaker than the new thermally-activated bonds, they could be useful for reversible bonding capability. Our previous work showed such magnetic bonds can be broken by anchoring and pulling modules apart [5]. However, such a method required electrostatic anchoring to apply pulling forces. We
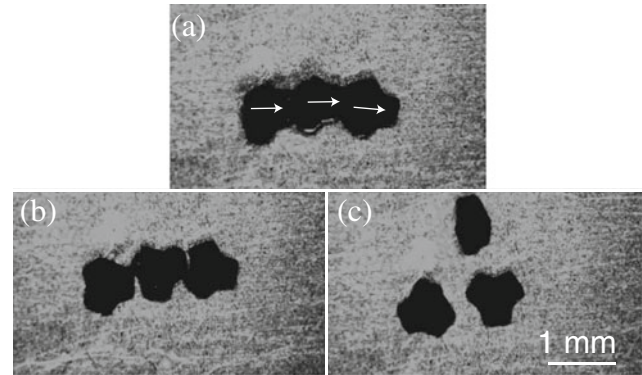

Fig. 11 Frames from a video showing three and four modules which can be disassembled by application of a disabling magnetic field pulse. **a** Three modules are held together using magnetic bonding. The assembly is mobile. Arrows indicate magnetization direction. **b** A field pulse is applied which magnetically disables the modules. **c** Modules are moved apart using moderately large magnetic fields. Here it is seen that disabled modules possess a small amount of residual magnetization. This is used to exert small magnetic forces and torques on individual modules to move them apart and prepare for future use. However, this residual magnetization can result in subsequent assembling of nearby modules. The exact value of this residual magnetization can be tuned through the magnetic pulse strength

now introduce the concept of magnetic disabling to such magnetic bonds for reversible control without the need for electrostatic anchoring. In this method, a magnetically-stable assembly is created, with the restriction that all magnetic modules must be assembled oriented in the same direction. To disassemble the group, all modules are magnetically disabled using a magnetic field pulse, in the manner of the previous section. Thus, the magnetic bonding force reduces to near-zero and the assembly is broken apart by small magnetic actuation forces and torques. At this point, individual modules can be re-enabled for re-use in further assemblies. The process is thus completely repeatable. A demonstration of this type of disassembly is shown in Fig. 11. Assembly in this case was performed by hand using tweezers. Magnetic modules in this study are identical to those used in the heat-assisted bonding study in this chapter, but without heat activation. This demonstrates that the principle could be used to create easily disassembled assemblies for reconfigurable magnetic micro-robotic tasks. Further investigations of the limits and usefulness of this technique could lead to a robust and simple disassembly method for magnetically-bonded assemblies.

5 Conclusions

In this paper, we have shown a comparison of several bonding methods for micro-scale modular robotics. As a reversible bonding method, we investigated magnetic attraction between modules, and as a stronger but non-reversible

bonding method we showed heat-activated metal solder and thermoplastic bonding methods. We showed solder and thermoplastic bonds activated by increasing the temperature through heating of the entire workspace, or as a proof-of-concept demonstration, through focused laser heating for faster heating/cooling in environments which may not be conducive to large heating elements. As a potential method for use in applications which lack line-of-sight view, we proposed the use of inductive heating to perform bonding with additional study required. The temperature increase required for bonding could be reduced through the use of different temperature sensitive materials with lower melting points. Bond strength was tested for a variety of different module styles for the thermoplastic bonds, and the temperatures required for solid bonding and cooling were investigated. As a demonstration, the magnetic modules were moved in a magnetic coil system as addressable microrobotic agents to remotely form a target structure from up to nine independent modules in a fluid environment accessible from only a small opening. Such an assembly method could potentially be used to form complex desired shapes in inaccessible small spaces for microfluidic manipulation or healthcare applications. As an additional bonding technique, we also demonstrated reversible magnetic bonding using a magnetic disabling technique for easy bond reversal. Future work will involve developing reversible adhesive bonds, and creating larger complex assemblies for tasks inside fluid channels. In addition, the formation of out-of-plane 3D assemblies will be investigated for applications such as in-situ heterogeneous tissue scaffold construction. Such applications may require reduced scale using fabrication methods such as flip-chip assembly [11] and biocompatibility through proper choice of materials and coatings.

References

1. Diller E, Floyd S, Pawashe C, Sitti M (2012) Control of multiple heterogeneous magnetic microrobots in two dimensions on nonspecialized surfaces. IEEE Trans Robot 28(1):172–182
2. Diller E, Giltinan J, Sitti M (2013) Independent control of multiple magnetic microrobots in three dimensions. Int J Robot Res 32(5):614–631
3. Diller E, Miyashita S, Sitti M (2012) Magnetic hysteresis for multi-state addressable magnetic microrobotic control. In: International conference on intelligent robots and systems, pp 2325–2331
4. Diller E, Miyashita S, Sitti M (2012) Remotely addressable magnetic composite micropumps. RSC Advances 2(9):3850–3856
5. Diller E, Pawashe C, Floyd S, Sitti M (2011) Assembly and disassembly of magnetic mobile micro-robots towards deterministic 2-D reconfigurable micro-systems. Int J Robot Res 30(14):1667–1680
6. Diller E, Zhang N, Sitti M (2013) Bonding methods for modular micro-robotic assemblies. In: International conference on robotics and automation, pp 2573–2578
7. Donald BR, Levey CG, Paprotny I, Rus D (2013) Planning and control for microassembly of structures composed of stress-engineered MEMS microrobots. Int J Robot Res 32(2):218–246
8. Gilpin K, Knaian A, Rus D (2010) Robot pebbles: one centimeter modules for programmable matter through self-disassembly. In: International conference on robotics and automation, pp 2485–2492
9. Hergt R, Dutz S (2007) Magnetic particle hyperthermia-biophysical limitations of a visionary tumour therapy. J Magn Magn Mater 311(1):187–192
10. Kummer M, Abbott J, Kratochvil B, Borer R, Sengul A, Nelson B (2010) Octomag: an electromagnetic system for 5-DOF wireless micromanipulation. IEEE Trans Robot 26(6):1006–1017
11. Mastrangeli M, Abbasi S, Varel C, Van Hoof C, Celis JP, Böhringer KF (2009) Self-assembly from milli- to nanoscales: methods and applications. J Micromech Microeng 19(8):083,001
12. Meeker D, Maslen E, Ritter R, Creighton F (1996) Optimal realization of arbitrary forces in a magnetic stereotaxis system. IEEE Trans Magn 32(2):320–328
13. Miyashita S, Diller E, Sitti M (2013) Two-dimensional magnetic micro-module reconfigurations based on inter-modular interactions. Int J Robot Res 32(5):591–613
14. Nelson BJ, Kaliakatsos IK, Abbott JJ (2010) Microrobots for minimally invasive medicine. Annu Rev Biomed Eng 12:55–85
15. Pawashe C, Floyd S, Sitti M (2009) Modeling and experimental characterization of an untethered magnetic micro-robot. Int J Robot Res 28(8):1077–1094
16. Rus D, Vona M (2001) Crystalline robots: self-reconfiguration with compressible unit modules. Auton Robot 10(1):107–124
17. Tabatabaei SN, Lapointe J, Martel S (2011) Shrinkable hydrogel-based magnetic microrobots for interventions in the vascular network. Adv Robot 25(8):1049–1067
18. Takeuchi M, Nakajima M, Kojima M, Fukuda T (2013) Handling of micro objects using phase transition of thermoresponsive polymer. J Micro-Bio Robot 8(2):53–64
19. Tolley MT, Krishnan M, Erickson D, Lipson H (2008) Dynamically programmable fluidic assembly. Appl Phys Lett 93(25):254,105
20. Tolley MT, Lipson H (2011) On-line assembly planning for stochastically reconfigurable systems. Int J Robot Res 30:1566–1584
21. White PJ, Yim M (2007) Scalable modular self-reconfigurable robots using external actuation. In: International conference on intelligent robots and systems, pp 2773–2778
22. White PJ, Yim M (2009) Reliable external actuation for full reachability in robotic modular self-reconfiguration. Int J Robot Res 29(5):598–612
23. Ye Z, Diller E, Sitti M (2012) Micro-manipulation using rotational fluid flows induced by remote magnetic micro-manipulators. J Appl Phys 112(6):064,912
24. Yim M, Shen WM, Salemi B, Rus D, Moll M, Lipson H, Klavins E, Chirikjian GS (2007) Modular self-reconfigurable robot systems. IEEE Robot Autom Mag 14(1):43–52
25. Yoshida E, Murata S, Kokaji S, Tomita K, Kurokawa H (2001) Micro self-reconfigurable modular robot using shape memory alloy. J Robot Mechatron 13:212–219
26. Zykov V, Mytilinaios E, Adams B, Lipson H (2005) Robotics: self-reproducing machines. Nature 435(7039):163–164